Performance Dependent Failure Criterion for Normal- and High-Strength Concretes

Paula Folino[1]; Guillermo Etse[2]; and Adrián Will[3]

Abstract: A new approach to describe the maximum strength criterion of concretes with different strength capacities is formulated. The proposed failure criterion incorporates the so-called "performance parameter" (β_P) that controls the dependence of the maximum strength on the concrete quality. To assure the feasibility of the solution procedure for any possible set of known data, different methods are proposed to determine β_P according to the available material data. The performance dependent strength criterion presented in this work is expressed in terms of the Haigh Westergaard stress coordinates and as a function of four material parameters that fully define the compressive and tensile meridians of the failure criterion. The variation of the shear strength between these two meridians follows an earlier elliptic interpolation. The proposal includes approximating functions that define the dependence of the above mentioned four material parameters on the two fundamental mechanical properties of concrete: the uniaxial compressive strength f'_c and the performance parameter β_P. The capability of the proposed criterion to predict peak stresses of both normal- and high-strength concretes is verified with experimental data available in the literature corresponding to uniaxial, biaxial, and triaxial compression tests.

DOI: 10.1061/(ASCE)EM.1943-7889.0000048

CE Database subject headings: Concrete; High-strength concrete; Failure modes; Parameters.

Introduction

The relevant knowledge evolution in concrete technology during the last decade has led to the development of concretes of very high compressive strengths characterized by mechanical properties that considerably differ from those of conventional or normal-strength concretes (NSCs). Presently, high-strength concretes (HSCs) are intensively used in the construction of high responsibility structures such as bridges, tall buildings, dams, etc. Nevertheless, and contrarily to the case of NSC, the mechanical behavior of HSC has still many unknown aspects, which are the subject of several ongoing experimental and numerical studies by the international research community.

Regarding the failure behavior of HSC and, moreover, the form of its maximum strength surface the available experimental evidence shows that they mainly depend on two fundamental material features: the uniaxial compressive strength (f'_c) and the mortar quality. However, no agreement was found so far on the indicator or parameter that best define the mortar or concrete quality.

Related to the formulation of concrete maximum strength criteria, most of the available proposals in the literature were developed for NSC and, due to the relevant differences, they cannot accurately predict the variation of the peak strength of HSC with the stress stage. As discussed in the section called "Review of Maximum Strength Criteria for Concrete" only a few empirical failure criteria have been proposed for HSC, see among others the contributions by Xie et al. (1995) and of Ansari and Li (1998). More limited were the attempts to develop failure criteria that are valid for a wide spectrum of concrete performances, as the one proposed by Seow and Swaddiwudhipong (2005). This strength criterion, although very easy to be implemented in computer programs, may lead to a poor accuracy as explained afterwards in the mentioned section.

In this work, a unified failure criterion for concrete of arbitrary performance is proposed that cover the entire spectrum of concrete quality from NSC to HSC. Depending on the material quality the proposed failure criterion leads to different forms of the maximum strength surface.

The novel failure criterion for concrete of arbitrary quality is based on the consideration of quadratic parabolas for the compressive and tensile meridians in the stress space expressed in terms of the Haigh Westergaard coordinates. Both parabolas have a joint apex on the hydrostatic axis so that only four parameters are required to completely define them. The innovative aspect is the inclusion of the water/binder (W/B) ratio as a fundamental property of the concrete mix controlling the material performance or quality that is objectively defined in terms of the so-called "performance parameter" (β_P). Thus, the four parameters defining the compressive and tensile meridians are expressed as functions of the uniaxial compressive strength and of the performance parameter in order to take into account the influence of the material quality in the form of the maximum strength surface. The dependence of the strength criterion on the Lode angle θ follows the elliptical function of the 5 parameter model by Willam and Warnke (1974).

To account for the different alternatives of known concrete

[1]Facultad de Ingeniería, Laboratorio de Materiales y Estructuras, Universidad de Buenos Aires (UBA), Las Heras 2214 (C1127AAR), Buenos Aires, Argentina (corresponding author). E-mail: pfolino@fi.uba.ar

[2]Facultad de Ingeniería, Laboratorio de Materiales y Estructuras (CONICET), Universidad de Buenos Aires, Las Heras 2214 (C1127AAR), Buenos Aires, Argentina. E-mail: getse@herrera.unt.edu.ar

[3]Facultad de Ciencias Exactas y Tecnología, Universidad Nacional de Tucumán (UNT), Av. Independencia 1800 (4000), Tucumán, Argentina. E-mail: awill@herrera.unt.edu.ar

Note. This manuscript was submitted on March 6, 2008; approved on September 18, 2008; published online on November 13, 2009. Discussion period open until May 1, 2010; separate discussions must be submitted for individual papers. This paper is part of the ***Journal of Engineering Mechanics***, Vol. 135, No. 12, December 1, 2009. ©ASCE, ISSN 0733-9399/2009/12-1393–1409/$25.00.

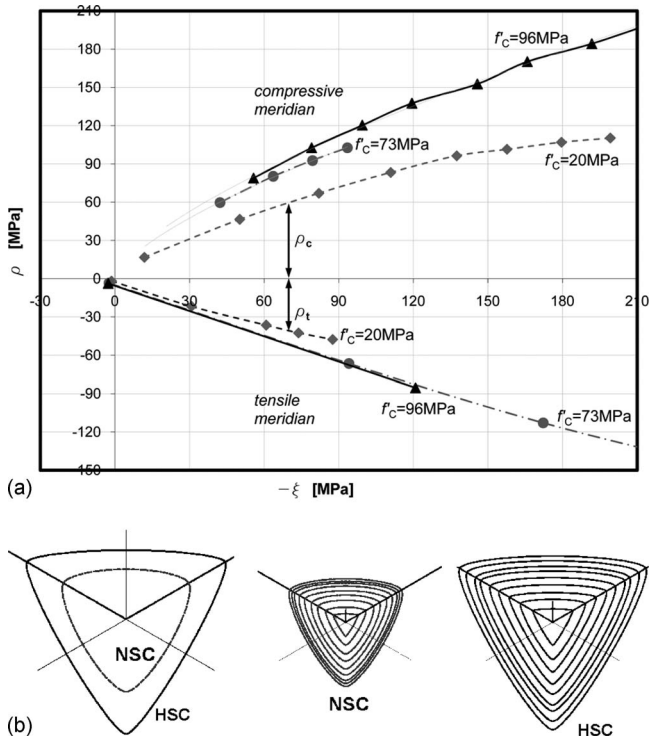

Fig. 1. NSC and HSC maximum strength curves—Data points: Chern et al. (1992); Candappa et al. (2001); Xie et al. (1995); Hampel and Curbach (2001): (a) meridian views; (b) deviatoric views

parameters, three different procedures for the evaluation of β_P were developed. One of them is based on empirical considerations while the others on numerical approximations. These numerical approximations are, on the one hand, an adaptive neurofuzzy inference system (ANFIS) and, on the other hand, a genetic algorithm (GA).

The comparisons between experimental results in terms of maximum strength surfaces and the corresponding numerical predictions included in this work demonstrate the capability and accuracy of the proposed maximum strength criteria for concretes of arbitrary performance.

Concrete Maximum Strength Features

Fig. 1(a) illustrates typical maximum strength curves of NSC and HSC on the compressive and tensile meridians while Fig. 1(b) shows their corresponding deviatoric views. These diagrams are depicted in terms of the Haigh Westergaard stress coordinates ξ, ρ, and θ as

$$\xi = \frac{I_1}{\sqrt{3}} \tag{1}$$

$$\rho = \sqrt{2J_2} \tag{2}$$

$$\cos(3\theta) = \frac{3\sqrt{3}}{2}\frac{J_3}{J_2^{3/2}} \tag{3}$$

thereby I_1=first invariant of the stress tensor $\underline{\underline{\sigma}}$; J_2=second invariant of the deviatoric stress tensor $\underline{\underline{s}}$; ($I_1=\delta_{ij}\sigma_{ij}$; $J_2=1/2s_{ij}s_{ij}$; $s_{ij}=\sigma_{ij}-1/3\delta_{ik}\sigma_{kj}$) and J_3=third invariant of the deviatoric stress tensor, $J_3=1/3s_{ij}s_{jk}s_{ki}$.

As follows from Eq. (2) ρ takes into account only the shear components of the deviatoric stress tensor in all Cartesian directions. Therefore, for a given ξ and θ, ρ defines the concrete strength for all shear stress components acting simultaneously.

The NSC curves in Fig. 1(a) shows that the shear measurement of concrete strength ρ progressively increases with the confining pressure and varies with the considered Lode angle θ. However, both the slope and the dependence on θ of the NSC maximum strength curves reduce for very high confinement levels.

With regard to the strength curves corresponding to HSC in Fig. 1(a), similarly to NSC, they show relevant dependence of the maximum ρ stress on both the confining pressure and the third stress invariant. The comparative analysis between the maximum strength curves of NSC and HSC leads to the following conclusions:

1. On the compressive meridian the HSC curves seems to have a steeper slope than those of NSC.
2. A linear increment of the uniaxial compressive strength from levels corresponding to NSC to those corresponding to HSC is not followed by a linear expansion of the maximum strength curve on the compressive meridian.
3. The concrete performance has more influence on the compressive meridians than on the tensile ones. Thus, the eccentricity $e=\rho_t/\rho_c$, being ρ_t and ρ_c the maximum shear strengths in the tensile and compressive meridians respectively, is clearly greater for NSC than for HSC. As an example, analyzing the data in Fig. 1(a) for $\xi=-60$ MPa, results in $\rho_t/\rho_c=0.69$ when $f'_c=20$ MPa (NSC), while $\rho_t/\rho_c=0.59$ when $f'_c=96$ MPa (HSC). This is illustrated in Fig. 1(b) by a comparison between the deviatoric views of NSC and HSC.

Due to experimental difficulties, there is a lack of data on concrete triaxial tests. Nevertheless, and for the purpose of the present work, a set of 18 triaxial test results performed in different laboratories on both NSC and HSC was considered. These data were extracted from the following literature:

- Ansari and Li (1998). Test samples: cylindrical 100 mm/200 mm (diameter/height).
- Candappa et al. (2001). Test samples: cylindrical 100 mm/200 mm (diameter/height).
- Chern et al. (1992). Test samples: cylindrical NX-core-sized 54 mm/108 mm (diameter/height).
- Hurlbut (1985). Test samples: cylindrical NX-core-sized 54 mm/108 mm (diameter/height).
- Imran and Pantazopoulou (1996). Test samples: cylindrical NX-core-sized 54 mm/108 mm (diameter/height).
- Lu (2005). Test samples: cylindrical 100 mm/150 mm (diameter/height).
- Sfer et al. (2002). Test samples: cylindrical 150 mm/300 mm (diameter/height).
- van Geel (1998). Test samples: cubes 100 mm/100 mm/100 mm.
- Xie et al. (1995). Test samples: cylindrical NX-core-sized 54 mm/108 mm (diameter/height).

In Fig. 2(a) the normalized ρ/f'_c versus ξ/f'_c failure meridians corresponding to the eighteen selected test sets are illustrated. It is important to note that relevant boundary conditions such as the geometry of the specimen, the age of concretes when the tests were performed, the stress paths, and the way the confinement was applied, do not agree among the different considered experimental tests in Fig. 2(a). Nevertheless, in all of them f'_c represents the uniaxial compressive strength at the time the triaxial test was performed.

To minimize the scatters due to the probe size and geometry

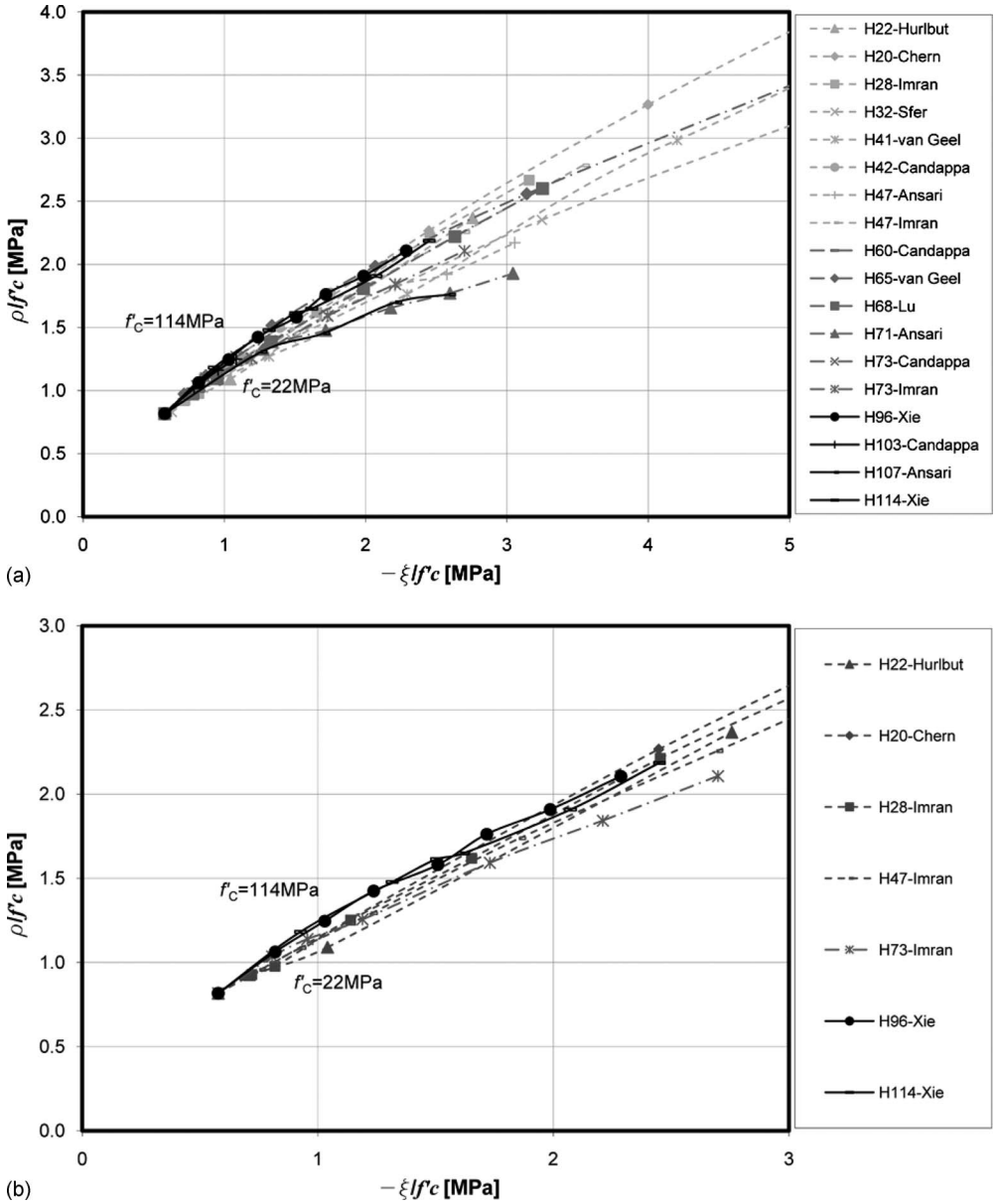

Fig. 2. Triaxial tests results—normalized plots: (a) different specimen sizes and geometries; (b) same specimen size and geometry

Fig. 2(b) shows those failure meridians corresponding to the experimental tests with the same specimen size and geometry. From the analysis of the plots in Figs. 2(a and b), some interesting conclusions follow:

1. The dispersion of the plots demonstrate that the simplification based on the consideration of one single normalized maximum strength surface for concretes of arbitrary performance is not accurate.
2. Concretes having similar uniaxial compressive strength may have different failure curves.
3. When considering experiment tests performed with concrete specimens of the same size and geometry the scatter of the failure meridians significantly reduces.
4. Even though the correlation is not the same for the different concretes considered in the experimental tests, in general the internal friction angle gradually and slightly increases with f'_c.
5. The shape of the maximum strength curve in the high confinement regime depends also on the followed stress path. While most of the experiments were done by first applying the lateral pressure and then increasing the axial displacement, some of them were obtained by simultaneously applying the lateral confinement and axial displacement (proportional loading). This last set of tests shows significant discrepancy in the shape of the failure surface; see Chern et al. (1992) and Ansari and Li (1998).

By stretching the rock mechanics features to concrete mechanics, we may also conclude that the internal friction angle increases with the concrete quality. In fact, most of the test results in Figs. 2(a and b) clearly demonstrate this effect.

Review of Maximum Strength Criteria for Concrete

Several triaxial failure criteria have been proposed for concrete. Some of them were originally developed for soils or for rocks and then further extended for concrete.

Following the evolution of the state of the art the most relevant

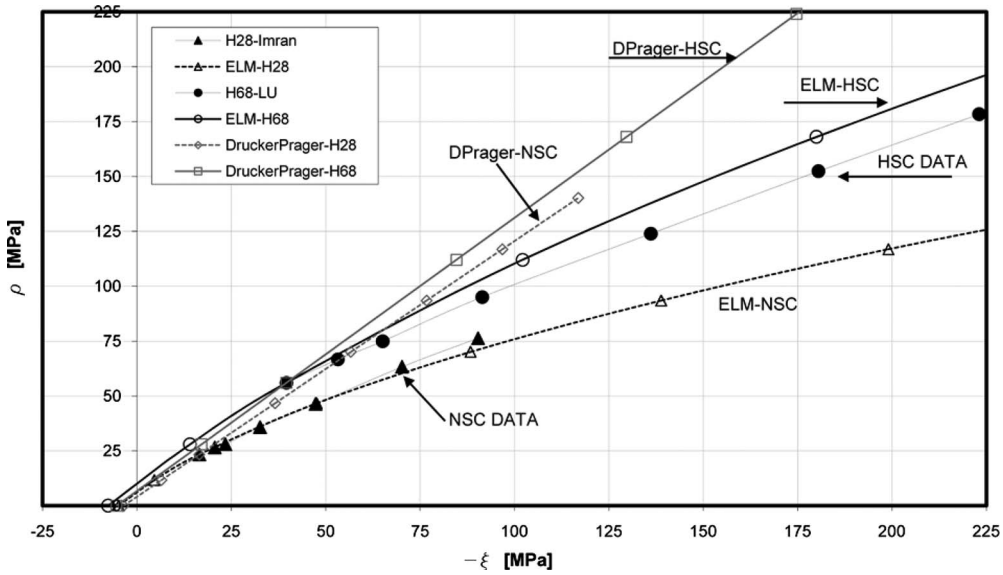

Fig. 3. Extended Leon and Drucker Prager's criteria predictions for NSC and HSC (data points: Imran and Pantazopoulou 1996; Lu 2005)

contributions are, among others, the criteria by Rankine (1876), Mohr-Coulomb (Mohr 1900), Mises-Schleicher [von Mises (1926)–Schleicher (1926)], Leon (1935), Drucker Prager (1952), Willam and Warnke (1974), Ottosen (1977), Hoek and Brown (1980), and Etse [extended Leon criterion—Etse (1992); Etse and Willam (1994)]. The respective material parameters of almost all the different models in the literature need to be specified for each concrete mix again. Moreover, as most of the proposed failure criteria were developed for NSC they do not have the appropriate accuracy to predict the maximum strength of HSC even by updating the material parameters. For example, the two parameters extended Leon criterion has a very good fitting to test results on NSC. However, it fails to adequately reproduce the failure envelope of HSC. This may be observed in Fig. 3 that illustrates the predictions of the maximum strength surfaces for both NSC and HSC, obtained with the extended Leon and the linear Drucker Prager's criteria. The five parameters model by Willam and Warnke was not considered in this analysis, as it requires results of triaxial tests for an appropriate calibration. This is a relevant shortcoming of this criterion.

To resolve the deficiencies of classical criteria to predict HSC maximum strength, new mathematical formulations have been suggested in the last years. Some of them are the proposals by Xie et al. (1995), Ansari and Li (1998), and Seow and Swaddiwudhipong (2005). Both the criteria by Xie et al. and Ansari and Li are characterized by empirical calibrations based on the results of triaxial tests performed by the writers on three different kinds of concrete strengths. Therefore, to extend its consideration to other concrete strengths, recalibration procedures based on new test results are required.

The criterion by Seow and Swaddiwudhipong takes into account an extensive experimental database to define a normalized maximum strength criterion valid for concretes of arbitrary qualities. The resulting surface is the one having the best fitting to the considered experimental data points. Although easy to be implemented the maximum strength criterion by Seow may lead in some cases, to a considerable loss of accuracy, as can be observed in Figs. 2(a and b).

From the review of the strength criteria for concrete in the literature, we conclude that further research is needed to obtain a unifying theory that accurately predicts failure criteria of concretes of arbitrary quality. This is the main purpose of the present proposal.

Performance Parameter for Concretes

There is no doubt that the uniaxial compressive strength f_c' is an essential property of concrete. On one hand, from a practical point of view it can be easily determined in laboratory tests and, on the other hand, provides relevant information on the concrete mechanical features.

Regarding the composite nature of concrete, its quality is controlled not only by the chemical properties but also by the physical and hydraulic properties of the mix and mix constituents. While the chemical properties are defined by the mortar composition, the hydraulic feature is basically the porosity of the mortar, and the physical ones are, among others, the shape and maximum size of the coarse aggregates. Thus, different mix proportions conduce to a different resulting composite material.

Until now, the uniaxial compressive strength f_c' has been considered as a synonymous of the concrete quality. Nevertheless, as different mix proportions, i.e., different chemical, physical and/or hydraulic properties, may lead to similar or same f_c' then, an additional parameter is required to quantify objectively the material quality. This additional or performance parameter should be related to f_c' and, should be able to describe the variation of the concrete quality from NSC to HSC in terms of the most relevant chemical, physical and hydraulic properties of the concrete mix.

To obtain a reliable definition of the performance parameter which allows accurate predictions of the material quality, more than 250 experimental data from the literature were evaluated in this work that are characterized by different mix proportions and related uniaxial compressive strengths. The considered experimental data belong to the range of uniaxial compressive strengths: $20\ \text{MPa} < f_c' < 120\ \text{MPa}$. The basic and common criteria considered for the selection of the experimental database are as follow: cylindrical samples 100 mm/200 mm, 28 days of curing under similar conditions, test performed at 28 days, cement Type I,

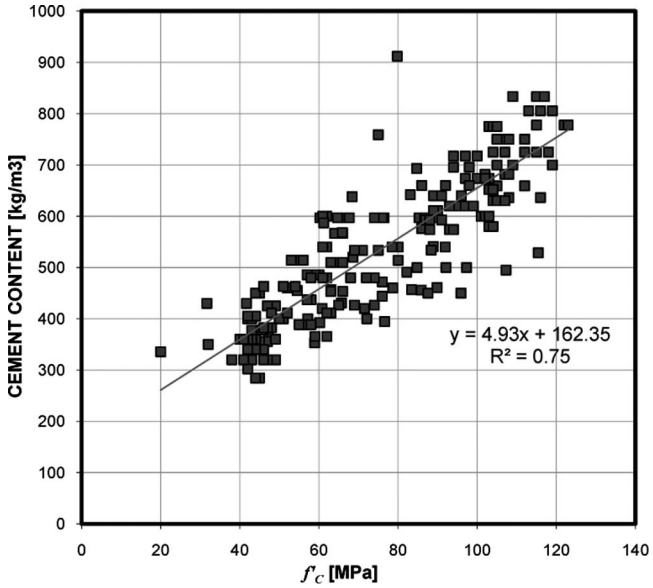

Fig. 4. Cement—f'_c

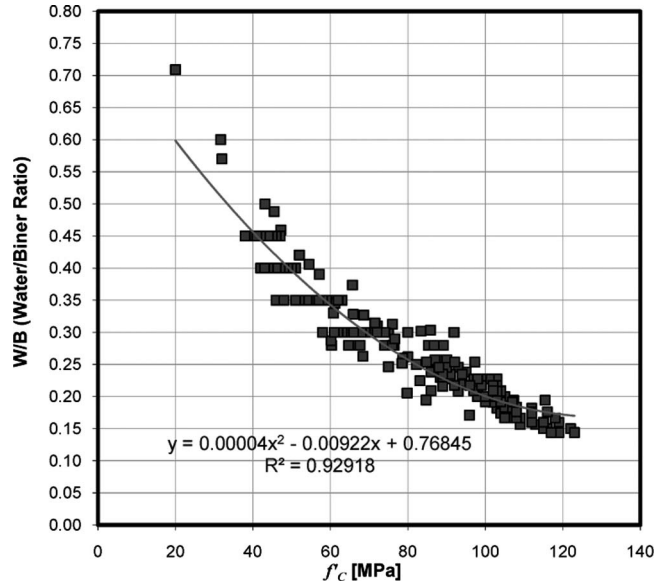

Fig. 5. W/B ratio—f'_c

similar loading rate, fiberless concrete mix, only natural sand as fine aggregate, and no air trained. Regarding the mineral admixtures, three cases are considered: no mineral admixtures; addition of silica fume; and addition of fly ash. (Note that these data correspond to uniaxial compression tests and do not coincide with the set of data used in the section called "Concrete Maximum Strength Features.") See Folino et al. (2007) for further details regarding the database.

By organizing the data in terms of the cement content and the related f'_c as indicated in Fig. 4, an overall increment of the cement content with f'_c can be recognized but with poor correlation. Therefore, it can be concluded that the cement content is not an appropriate parameter to define the quality of concrete. Several other properties of the concrete mix were also evaluated, such as water content, silica fume content, fly ash content, superplasticizer content, coarse aggregate content, fine aggregate content, total volume of aggregates, relative volume of aggregates, and maximum coarse aggregate size. It was found that although most of them follow a tendency, a very poor correlation is obtained. Thus, it was concluded that none of them is clearly related to the concrete quality.

However, by relating f'_c with the W/B ratio, whereby the binder takes into account not only the cement content but also eventual mineral admixture contents such as silica fume and/or fly ash, a defined correlation is obtained (see Fig. 5). It is important to note that the well-known Abrams law proposed in 1918 when only NSC existed already takes into account the relation between f'_c and the water/cement ratio. In this sense, the plot in Fig. 5 can be understood as an extension of the Abrams law to encompass both NSC and HSC when the pure cement content is replaced with the binder content.

Then, it is concluded that the most effective set of parameters to objectively quantify the quality of concrete is the one composed by f'_c and the W/B. Consequently, the so-called *performance parameter* "β_P" is defined as

$$\beta_P = \frac{1}{1000}\frac{f'_c}{(\mathrm{W/B})} \quad f'_c \text{ in (MPa)} \tag{4}$$

where W=water content (kg/m^3) and B=binder content (kg/m^3), constituted by the sum of the cement and the mineral admixtures contents (kg/m^3).

In Fig. 6 the resulting dependence of the performance parameter β_P on f'_c, corresponding to all the different considered experimental data, is plotted. Note that for a given value of f'_c different β_P may arise depending on the particular W/B ratio. The β_P-f'_c relation in Fig. 6 plays a relevant role in the formulation of the performance dependent criterion for concrete of arbitrary quality proposed in this paper in terms of the uniaxial compressive strength and of the performance parameter.

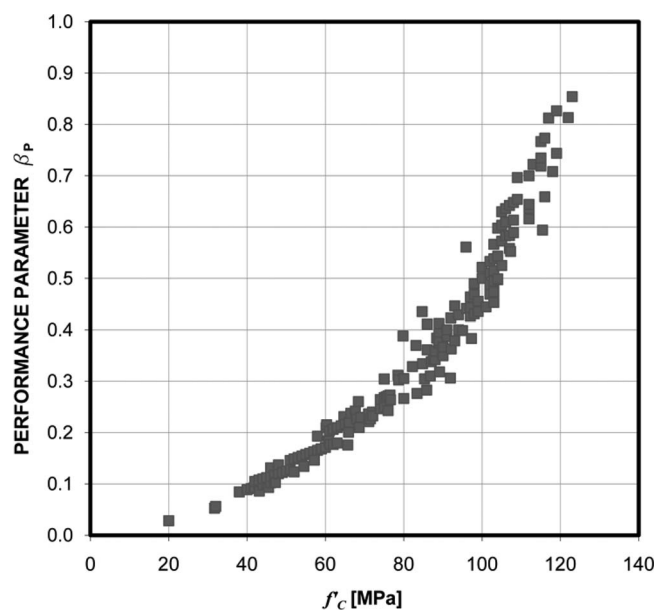

Fig. 6. Variation form of the performance parameter β_P with f'_c

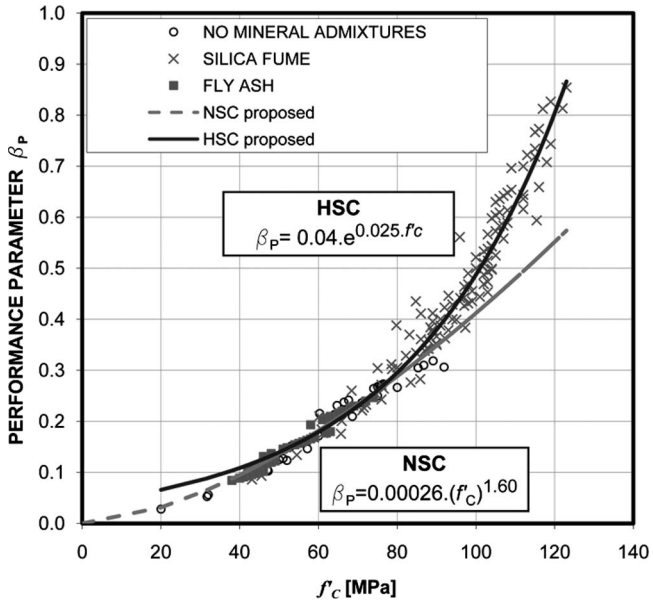

Fig. 7. Proposed variation form of the mean value of the performance parameter β_P with f'_c

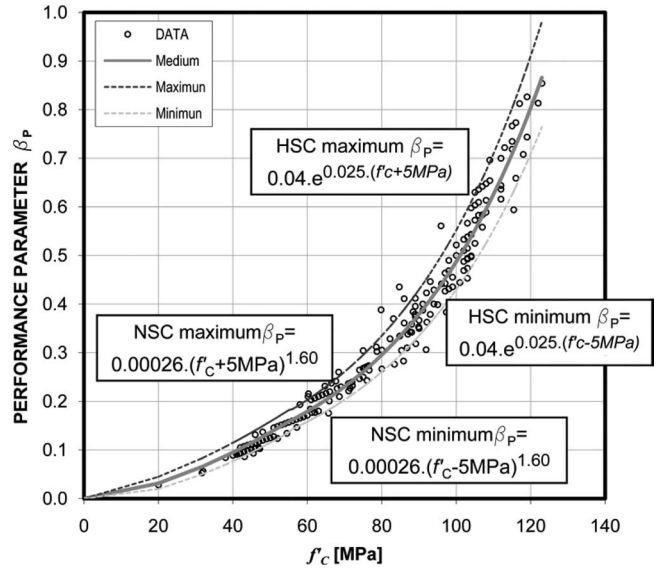

Fig. 8. Proposed variation forms of the upper and bottom limits of β_P with f'_c

Evaluation Strategies of the Performance Parameter

The evaluation of the proposed performance parameter may be a very difficult task. This is due to the fact that the W/B ratio is not always known in advance. Three possible situations may be distinguished for the evaluation of β_P as follow:

- Case 1—both, the concrete mixture and f'_c are known;
- Case 2—the concrete mixture is unknown and cannot be evaluated while f'_c is known; and
- Case 3—the unknown concrete mixture can be evaluated following numerical methods, while f'_c is known.

It is clear that in case 1 the W/B ratio can be easily calculated from the known concrete mixture. Then as f'_c is also known, β_P is determined with Eq. (4).

Case 2 is the one corresponding to an existing concrete. So, the uniaxial compressive strength can be evaluated by means of destructive or nondestructive tests. However, the composition of the concrete mixture and, therefore, the W/B ratio are unknown. To bypass the dependence of β_P on the W/B ratio, a relation between the performance parameter and f'_c is proposed in this work that is useful in this Case 2. Thus, β_P and, therefore, the concrete performance level can be determined from the only available material parameter f'_c. The dependent function of β_P in terms of f'_c can be obtained from the plot in Fig. 6. The detailed observation of the β_P-f'_c relation in this figure leads to the conclusion that the dependent function has a potential form when $f'_c < 55$ MPa while it has an exponential form when $f'_c > 80$ MPa. (See Fig. 7.)

As can be observed in Fig. 7 the β_P-f'_c relation is not single valued due to the dependence of β_P on both f'_c and W/B. In this work an upper and lower limiting curves representing the variation range of β_P in terms of f'_c are proposed. These limiting curves content the set of maximum and minimum values of β_P for all possible f'_c depending on W/B. (See Fig. 8). The upper $\beta_{P\,\max}$ and lower $\beta_{P\,\min}$ limits of the performance parameter are defined as

$$\beta_{P\,\max} = \begin{cases} (2.60E-4)(f'_c+5)^{1.60} & \text{when } f'_c \le 55 \text{ MPa} \\ (4.00E-2)e^{(2.5E-2)(f'_c+5)} & \text{when } f'_c > 55 \text{ MPa} \end{cases} \tag{5}$$

$$\beta_{P\,\min} = \begin{cases} (2.60E-4)(f'_c-5)^{1.60} & \text{when } f'_c \le 55 \text{ MPa} \\ (4.00E-2)e^{(2.5E-2)\cdot(f'_c-5)} & \text{when } f'_c > 55 \text{ MPa} \end{cases} \tag{6}$$

with f'_c in (MPa).

Case 3 corresponds to the most common situation whereby the concrete is to be designed. The evaluation of the concrete mixture composition is performed in accordance with the particular f'_c that is expected to be reached. For this evaluation, two numerical procedures are proposed in this work: an ANFIS and, a GAs system (GAS). These procedures are described in the next sections.

Adaptive Neurofuzzy Interface System Procedure for the Prediction of f'_c

The ANFIS is a particular type of networks that accepts fuzzy input variables. They have been successfully applied to model-free prediction based on historical data such as stock market, weather, and river level forecasts as well as to a wide range of industrial and military problems. They are particularly suitable to work with low precision databases that are characterized by low linearity, highly complex relations and/or high noise levels that are frequently found in practical situations. They require appropriate treatment of the input data, and massive amounts of processing.

In the present case, the proposed ANFIS defines an iterative procedure to evaluate the uniaxial compression strength f'_c corresponding to a given or known concrete mixture. The procedure starts by assuming a concrete mix proportion and calculating f'_c by means of the ANFIS (Fig. 9). If the obtained f'_c is acceptable, the mix proportion is adopted. Otherwise, a different mix proportion is considered. Details of the proposed ANFIS are given in Folino et al. (2007). This numerical tool was developed on the

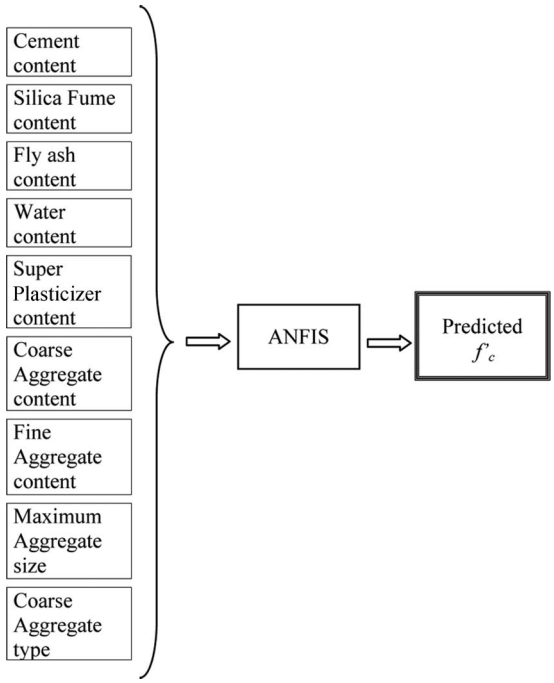

Fig. 9. ANFIS system

basis of 254 data taken from the available literature. The network considers 9 input variables and one output variable. It accurately predicts the uniaxial compression strength f'_c corresponding to the considered concrete mixture.

Genetic Algorithm System for the Prediction of a Set of Concrete Mixes

GAs are a class of evolutionary algorithms used in heuristic optimization. Evolutionary algorithms are mainly based on the concept of Darwin´s evolution. That is, evolution over time of a population and survival of the fittest in order to find the extreme value (maximum or minimum) of a function. They have been successfully applied to many real life problems and are particularly suitable for complex, nondifferentiable problems. They are also suitable to be applied in problems characterized by many local maximums whereby a global near-optimum is needed. We used in this work a modification (niching GA), based on the biological idea of speciation and niching (in nature, different species evolve in order to occupy ecological niches that are not occupied by other species). This allows the GA to attain and preserve not only one global near optimal, but a complete list of other good solutions, which is the objective of the work.

It is important to notice that the initial population is randomly

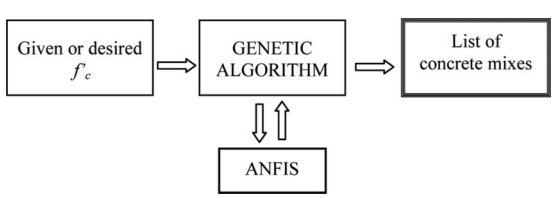

Fig. 10. GAS

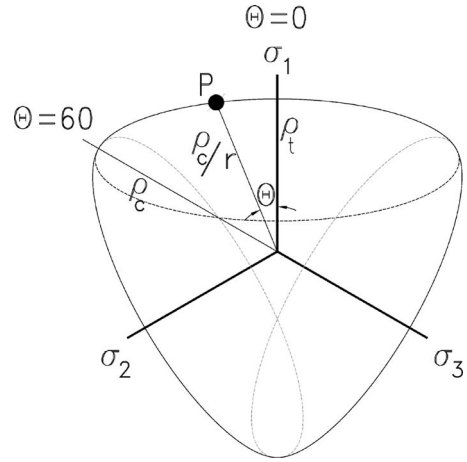

Fig. 11. Elliptic description in the deviatoric plane

generated and, as a consequence, a lot of random steps need to be processed. So, a significant effort and processing time is devoted to ensure agreement among the obtained results.

In this research a GAS was developed that includes the ANFIS network as a part of the GA fitness function. As a result of the application of the GAS, see Fig. 10, a list of possible concrete mixtures corresponding to the given or desired f'_c is obtained. It allows introducing some constraints in the concrete mixture such as no silica fume, no fly ash, or to fix some of the variables that are known from the beginning (i.e., type of coarse aggregate). By selecting one choice of the list of possible concrete mixtures obtained by the GAS a realistic knowledge of the concrete content proportions is achieved. Details of the GAS are being published in a separated paper by the writers.

Performance Dependent Failure Criterion for Concretes of Arbitrary Quality

In this section, a novel failure surface of concretes of arbitrary strength performances is presented. The proposed concrete strength criterion is based on the 5-parameters criterion by Willam and Warnke (1974).

The concrete failure condition in the Haigh Westergaard stress coordinates (ξ, ρ, θ) can be expressed as

$$F_{(\xi,\rho,\theta,f'_c,\beta_P)} = \frac{\rho}{\rho^*} - 1 = 0 \Rightarrow \rho = \rho^* \tag{7}$$

with ρ^*=shear strength that varies with the Lode angle θ according to the elliptic interpolation by Willam and Warnke (1974) between the compressive and the tensile meridians

$$\forall \quad 0° \leq \theta \leq 60° \Rightarrow \rho^* = \frac{\rho_c}{r} \tag{8}$$

with

$$r = \frac{4 \cdot (1 - e^2) \cdot \cos^2 \theta + (2 \cdot e - 1)^2}{2 \cdot (1 - e^2) \cdot \cos \theta + (2 \cdot e - 1) \cdot \sqrt{4 \cdot (1 - e^2) \cdot \cos^2 \theta + 5 \cdot e^2 - 4 \cdot e}} \tag{9}$$

and e=eccentricity, defined as the ratio between the tensile and the compressive shear strength

$$e = \frac{\rho_t}{\rho_c} \tag{10}$$

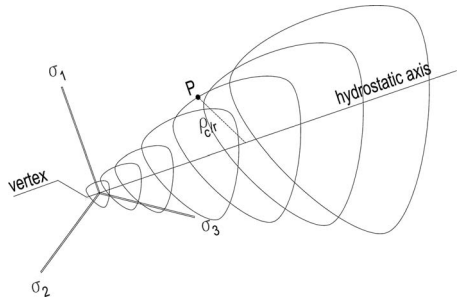

Fig. 12. 3D view of the deviatoric planes

The elliptic approximation of ρ^* assures a C1-type continuity of the failure surface in the deviatoric plane (see Figs. 11 and 12). From Eqs. (9) and (10), follows that $r=1$ when $\theta=\pi/3$, while $r=\rho_c/\rho_t$ when $\theta=0°$.

In the proposed failure criterion for concrete of arbitrary quality the compressive and the tensile meridians are considered to be quadratic polynomials of the general form

$$A_i \cdot \bar{\rho}^2 + B_i \cdot \bar{\rho} + C_i \cdot \bar{\xi} - 1 = 0 \tag{11}$$

with the normalized stress coordinates $\bar{\rho}=\rho/f_c'$; $\bar{\xi}=\xi/f_c'$ and the subindexes $i=c,t$ denoting the coefficients of the compressive and tensile meridians, respectively. Therefore, a total of six coefficients are involved.

By assuming that all the meridians have a common vertex on the $\bar{\rho}$ axis, then $C_c=C_t=C$. In this work, it is also assumed that the coefficient defining the quadratic dependence of the maximum strength surface on the normalized shear stress coordinate $\bar{\rho}$ does not depend on θ, and therefore, remains unchanged in the compressive and tensile meridians, i.e., $A_c=A_t=A$. Then, from Eq. (11) the following expressions of the compressive and tensile meridians are obtained

$$\theta = \frac{\pi}{3} \Rightarrow A \cdot \bar{\rho}_c^2 + B_c \cdot \bar{\rho}_c + C \cdot \bar{\xi} - 1 = 0 \tag{12}$$

$$\theta = 0 \Rightarrow A \cdot \bar{\rho}_t^2 + B_t \cdot \bar{\rho}_t + C \cdot \bar{\xi} - 1 = 0 \tag{13}$$

involving a total of four independent coefficients (A, B_c, B_t, and C). For their evaluation, the following four independent auxiliary conditions are considered (see Fig. 13):

- Condition 1. The peak stress's shear component corresponding to the uniaxial compression test belongs to the compressive meridian. The Haigh Westergaard coordinates of this peak stress are: $\theta=\pi/3$, $\bar{\xi}=-\sqrt{3}/3$, and $\bar{\rho}_c=\sqrt{2}/\sqrt{3}$.

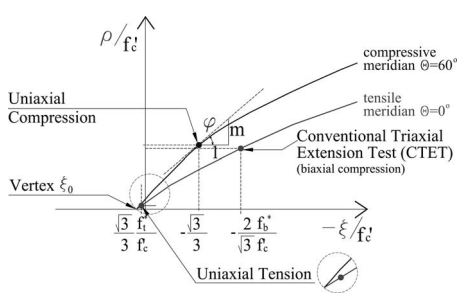

Fig. 13. Imposed conditions on the compressive and tensile meridians

- Condition 2. The tangent to the compressive meridian on the peak stress's shear component corresponding to the uniaxial compression test is defined as: $\partial(\bar{\rho})/\partial(\bar{\xi})=m$, being m a material property. Note: in case of linear polynomials defining the compressive and tensile meridians, m would coincide with the classical friction angle.
- Condition 3. The shear component of the peak stress state corresponding to the uniaxial tensile test belongs to the tensile meridian. The Haigh Westergaard coordinates of this peak stress are: $\theta=0$, $\bar{\xi}=\sqrt{3}\cdot\alpha_t/3$, and $\bar{\rho}_t=\sqrt{2}\cdot\alpha_t/\sqrt{3}$. Thereby is α_t the strength ratio defined as: $\alpha_t=f_t^*/f_c'$, with f_t^*, the uniaxial tensile strength.
- Condition 4. The shear component of the peak stress state corresponding to the Conventional Triaxial Extension Test (CTET) characterized by the cylindrical stress state $\sigma_z=0$; $\sigma_r=\sigma_\theta<0$ belongs to the tensile meridian. The Haigh Westergaard coordinates of this peak stress are: $\theta=0$, $\bar{\xi}=-2\cdot\alpha_b/\sqrt{3}$, and $\bar{\rho}_b=\sqrt{2}\cdot\alpha_b/\sqrt{3}$, being α_b the strength ratio defined as: $\alpha_b=f_b^*/f_c'$, and f_b' the peak lateral confining pressure of the CTET under zero axial stress.

By replacing the considered auxiliary conditions in Eqs. (12) and (13), a system of four linear equations is obtained (see Appendix for further details)

$$(1) \Rightarrow \frac{2}{3}\cdot A + \sqrt{\frac{2}{3}}\cdot B_c - \frac{1}{\sqrt{3}}\cdot C - 1 = 0 \tag{14}$$

$$(2) \Rightarrow 2\cdot\sqrt{\frac{2}{3}}\cdot A + B_c - \frac{1}{m}\cdot C = 0 \tag{15}$$

$$(3) \Rightarrow \frac{2}{3}\cdot\alpha_t^2\cdot A + \sqrt{\frac{2}{3}}\cdot\alpha_t\cdot B_t + \frac{\alpha_t}{\sqrt{3}}\cdot C - 1 = 0 \tag{16}$$

$$(4) \Rightarrow \frac{2}{3}\cdot\alpha_b^2\cdot A + \sqrt{\frac{2}{3}}\cdot\alpha_b\cdot B_t - \frac{2\cdot\alpha_b}{\sqrt{3}}\cdot C - 1 = 0 \tag{17}$$

The four unknowns can be obtained by solving Eqs. (14)–(17) with

$$A = -\frac{3}{2}\left\{1 + \frac{(m-\sqrt{2})(1-\alpha_b\alpha_t)(\alpha_b-\alpha_t)}{\alpha_b\alpha_t[(m-\sqrt{2})(\alpha_b-\alpha_t)+3m]}\right\} \tag{18}$$

$$B_c = \sqrt{3}\left\{\sqrt{2} + \frac{(\sqrt{2}m-1)(1-\alpha_b\alpha_t)(\alpha_b-\alpha_t)}{\alpha_b\alpha_t[(m-\sqrt{2})(\alpha_b-\alpha_t)+3m]}\right\} \tag{19}$$

$$B_t = \sqrt{\frac{3}{2}}\left\{\frac{1+\alpha_t^2}{\alpha_t} + \frac{[(m-\sqrt{2})\alpha_t-m](1-\alpha_b\alpha_t)(\alpha_b-\alpha_t)}{\alpha_b\alpha_t[(m-\sqrt{2})(\alpha_b-\alpha_t)+3m]}\right\} \tag{20}$$

$$C = \sqrt{3}m\frac{(1-\alpha_b\alpha_t)(\alpha_b-\alpha_t)}{\alpha_b\alpha_t[(m-\sqrt{2})(\alpha_b-\alpha_t)+3m]} \tag{21}$$

From Eqs. (7) and (8) follows that $\overline{\rho_c}=r\cdot\overline{\rho^*}$. Then, by replacing $\overline{\rho_c}$ in Eq. (12), the general form of the performance dependent failure criterion proposed in this paper is obtained

$$F = A\cdot r^2\cdot\overline{\rho^*}^2 + B_c\cdot r\cdot\overline{\rho^*} + C\cdot\bar{\xi} - 1 = 0 \tag{22}$$

Eqs. (18)–(21) express the coefficients A, B_c, B_t, and C in terms of four material parameters: (a) the uniaxial compressive

strength f'_c; (b) the tangent m to the compressive meridian at the $\bar{\xi}-\bar{\rho}$ coordinates corresponding to the peak stress state of the uniaxial compression test; (c) the uniaxial tensile strength ratio α_t; and (d) the biaxial compressive strength ratio α_b.

As indicated in the section called "Performance Parameter for Concretes" to completely define the quality of the particular concrete under consideration two material parameters are required, the uniaxial compressive strength f'_c and the performance parameter β_P. Thus, to account for the material quality influence in the present formulation of concrete maximum strength criterion the three controlling material parameters beside f'_c, i.e., m, α_t, and α_b, are defined in terms of β_P by means of numerical approximations. These functions are as follows:

1. Proposed m-β_P relation: although m does not fully agree with the classical definition of material friction they are closely related. Thus, similarly to the case of the frictional parameter it is assumed that the tangent m also increases with the concrete performance. This increment is considered as follows:

$$m = 1.05 \cdot \beta_P^{0.05} \tag{23}$$

The procedure for the evaluation of the m parameter is as follows: first, the performance parameter β_P is obtained as it was explained in the section called "Evaluation Strategies of the Performance Parameter." For example, if f'_c=80 MPa then from Eqs. (5) and (6) the corresponding upper and lower limits of β_P are obtained ($\beta_{P\,\max}$=0.335; $\beta_{P\,\min}$=0.261). By selecting the mean value, results β_P=0.298, and by means of Eq. (23), m=0.99 (44.7°). The upper and lower limiting values of β_P would lead to the friction angles 44.8 and 44.5°, respectively. Observe that if the W/B ratio is known, then β_P could be determined directly by means of Eq. (4).

2. Proposed α_t-β_P relation

$$\alpha_t = \frac{f_t^*}{f'_t} = \frac{6.70 \cdot \beta_P^{0.27}}{f'_c} \quad f_t^*, f'_c \text{ in (MPa)} \tag{24}$$

3. Proposed α_b-β_P relation: the biaxial compressive strength ratio α_b is defined in terms of α_t and β_P as

$$\alpha_b = \frac{f_b^*}{f'_b} = (1.21 \cdot k_b + 1.50 \cdot \alpha_t)$$

$$k_b \begin{cases} \beta_P \geq \beta_{P\,\max} \rightarrow k_b = 0.89 \\ \beta_{P\,\min} \leq \beta_P \leq \beta_{P\,\max} \rightarrow k_b = 1 - 0.11\left[\dfrac{\beta_P - \beta_{P\,\min}}{\beta_{P\,\max} - \beta_{P\,\min}}\right] \\ \beta_P \leq \beta_{P\,\min} \rightarrow k_b = 1 - 0.125\left[\dfrac{\beta_P - \beta_{P\,\min}}{\beta_{P\,\max} - \beta_{P\,\min}}\right] \end{cases} \tag{25}$$

where $\beta_{P\,\max}$ and $\beta_{P\,\min}$ are obtained from Eq. (5) or (6).

Eqs. (24) and (25) play a very important role in the proposed formulation for concrete maximum strength criterion as the material parameters f'_t and f'_b cannot be obtained from standard tests. Moreover, the scarce test results available in the literature correspond to test programs involving uniaxial tensile tests or biaxial compressive tests, but very rarely to both of them. Herein it is assumed a dependence of the tensile and compressive strength ratios on the performance parameter, allowing the possibility to have two concretes with the same f'_c but different f'_t and f'_b, which agrees with the available test results. Notice that to distinguish the proposed values from the "real" ones, an asterisk has been introduced. Various writers have reported an inflection point at about f'_c=55 MPa in the f'_t versus f'_c relation. This issue was also taken into account in the proposed function for α_t. In conclusion, the material properties m, α_t and α_b can be evaluated with Eqs. (23)–(25), or alternatively, from experimental tests.

To assure a stable behavior, the surface must not present inflection points (Drucker's postulate), and therefore it must satisfy convexity. Experimental evidence demonstrates that the concrete maximum strength surface remains convex (no inflection point) even being the uniaxial tensile strength much smaller than the compressive one.

The convexity of the proposed maximum strength surface in the meridian view is assured by the parabolic proposed dependence function of $\bar{\xi}$ in terms of $\bar{\rho}$. In the deviatoric plane the convexity of the failure surface is controlled by the auxiliary condition

$$0.50 \leq e \leq 1.00 \tag{26}$$

of the eccentricity e that follows from the elliptic approximation of the shear strength accordingly to Willam and Warnke (1974). The auxiliary condition for convexity in Eq. (26) leads to a coupling between the material parameters m, α_t and α_b as can be observed in the following equations.

From the relations in Eqs. (12) and (13), it results

$$A \cdot \overline{\rho_c}^2 + B_c \cdot \overline{\rho_c} = A \cdot \overline{\rho_t}^2 + B_t \cdot \overline{\rho_t} \tag{27}$$

After some algebra follows:

$$\Rightarrow A \cdot e^2 \cdot \overline{\rho_c} + B_t \cdot e - A \cdot \overline{\rho_c} - B_c = 0 \tag{28}$$

$$\Rightarrow A \cdot \overline{\rho_c} = \frac{-B_t \cdot e + B_c}{(e^2 - 1)} \tag{29}$$

Considering the extreme values for the compressive shear strength $\overline{\rho_c}$

$$\Rightarrow \overline{\rho_c} \rightarrow \infty (e^2 - 1) \rightarrow 0 \Rightarrow e \rightarrow 1 \tag{30}$$

$$\Rightarrow \overline{\rho_c} \rightarrow 0 \Rightarrow (-B_t e + B_c) \rightarrow 0 \Rightarrow e \rightarrow \frac{B_c}{B_t} \tag{31}$$

From Eq. (30) follows that in the high confinement regime ($\bar{\rho} \rightarrow \infty$) the deviatoric view of the surface approximates a circle, indicating constant shear strength for all possible Lode angles, similarly to the Drucker Prager criterion.

From Eq. (31) and the auxiliary condition in Eq. (26) follows the coupling condition between B_c and B_t

$$1.00 \geq \frac{B_c}{B_t} \geq 0.50 \tag{32}$$

By replacing the explicit expressions of B_c and B_t from Eqs. (19) and (20) in Eq. (32) we obtain

$$B_c \geq 0.50 \cdot B_t \Rightarrow \sqrt{3}\left\{\sqrt{2} + \frac{(\sqrt{2}m - 1)(1 - \alpha_b\alpha_t)(\alpha_b - \alpha_t)}{\alpha_b\alpha_t[(m - \sqrt{2})(\alpha_b - \alpha_t) + 3m]}\right\}$$
$$\geq \frac{1}{2}\sqrt{\frac{3}{2}}\left\{\frac{1 + \alpha_t^2}{\alpha_t} + \frac{[(m - \sqrt{2})\alpha_t - m](1 - \alpha_b\alpha_t)(\alpha_b - \alpha_t)}{\alpha_b\alpha_t[(m - \sqrt{2})(\alpha_b - \alpha_t) + 3m]}\right\} \tag{33}$$

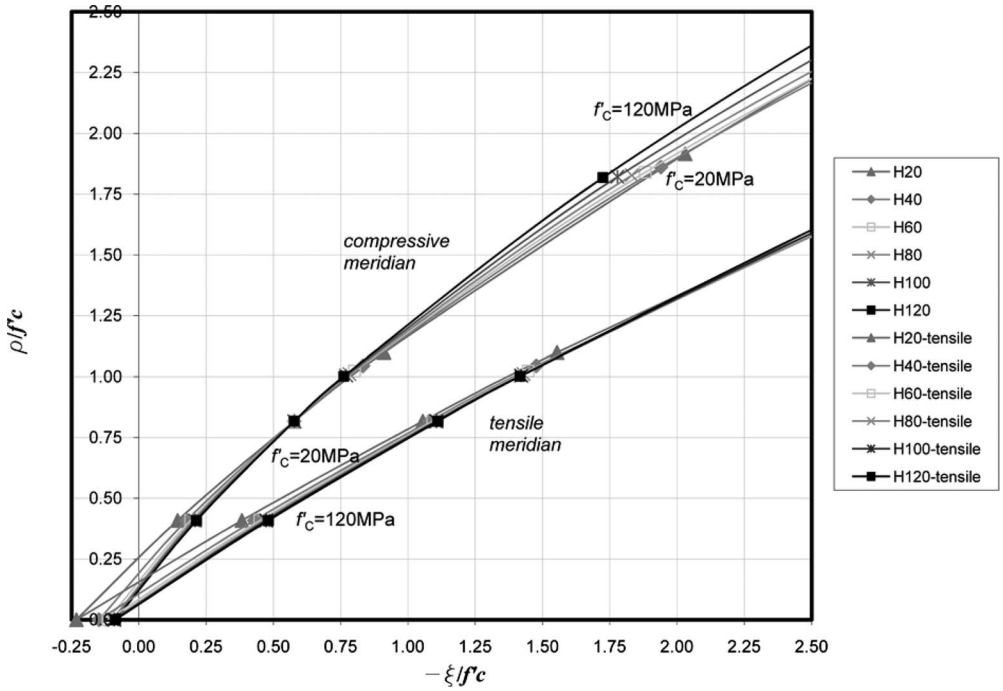

Fig. 14. Predictions of maximum strength compressive and tensile meridians in normalized stress coordinates for different concrete performances

After some algebra follows

$$\left[(\sqrt{2}-m)\alpha_t\frac{1+\alpha_t^2-4\alpha_t}{\alpha_t[m(5-\alpha)+\sqrt{2}(\alpha_t-2)]}-\alpha_t\right]\cdot\alpha_b^2+\left[1+\alpha_t^2+[(m-\sqrt{2})\alpha_t^2-3m\alpha_t]\frac{1+\alpha_t^2-4\alpha_t}{\alpha_t[m(5-\alpha_t)+\sqrt{2}(\alpha_t-2)]}\right]\cdot\alpha_b-\alpha_t\geq 0 \tag{34}$$

which represents the coupling due to the convexity condition between the material parameters m, α_t and α_b.

Then the procedure is as follow. Once the parameters m, α_t and α_b are determined from Eqs. (23)–(25) or, alternatively from experiment tests, the inequality (34) must be verified. If it is not fulfilled, two of the three material parameters are set fixed while the third one is recalculated with Eq. (34).

Figs. 14 and 15 illustrate the compressive and tensile meridians of the proposed failure criterion for different concrete performances. Fig. 16 shows 3D views of the proposed performance dependent failure criterion for different concrete qualities.

The proposed performance dependent strength criterion is

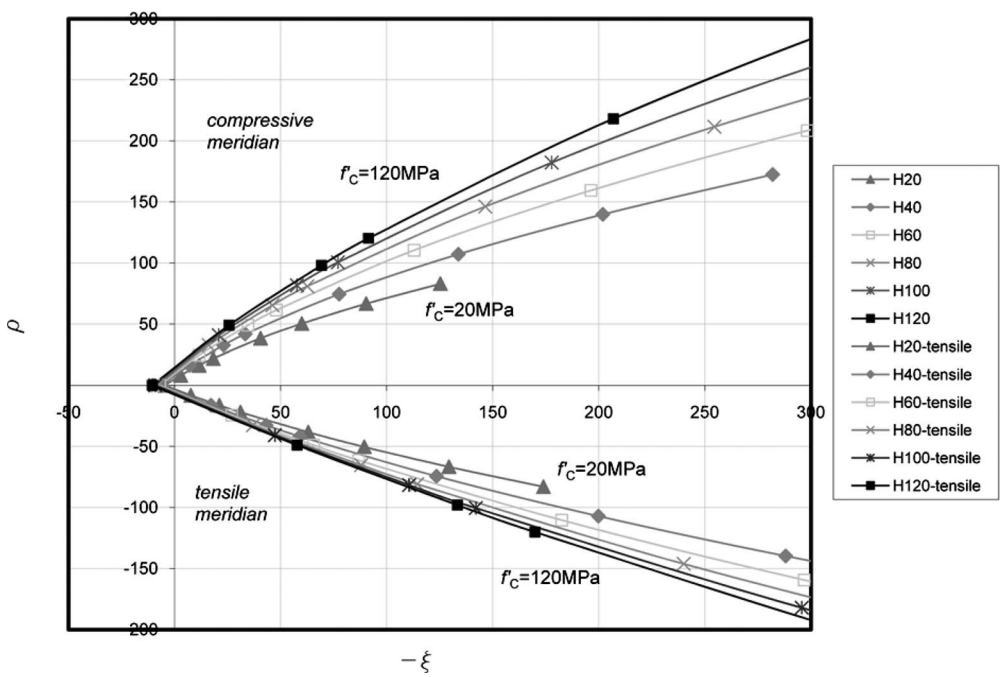

Fig. 15. Predictions of the compressive and tensile meridians for different concrete performances

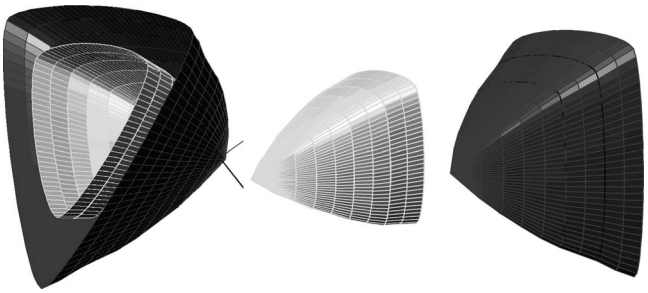

Fig. 16. NSC and HSC failure surfaces 3D views

valid for plain concrete with uniaxial compressive strength varying from 15 to 140 MPa. Due to the lack of concrete triaxial tests in the very high confinement regime, the recommended limit of applicability of the proposed failure criterion is defined by the normalized pressure level of $|\xi/f_c'| \leq 6$. For larger confining pressures, a "cap" surface needs to be introduced.

Numerical Validation

In this section, the predictive capabilities of the proposed maximum strength criterion for concretes of arbitrary qualities are evaluated. To this end, three sets of available data are considered. In all of them, the uniaxial compression strength f_c' is known. In the first case, the concrete mixture is known too. In the second case, the concrete mixture is unknown and cannot be defined due to the lack of data. In the third case, the concrete mixture is not known and is defined by means of the proposed numerical algorithms.

Example Case 1—The Concrete Mixture and f_c' Are Known

The predictions of the maximum strength curve for the experimental triaxial compression tests in Fig. 2(a) were evaluated. The performance parameter β_P was determined with Eq. (4) based on the known values of f_c' and W/B. The results in terms of the predicted maximum strength curve and the comparison with the experimentally obtained strengths are depicted in Figs. 17–22 for the different cases. These figures include the minimum and maximum relative errors obtained with the predictions, being the relative error evaluated as: Error=(Predicted value-Test Result)/Test result

Analogously, the experimental tests performed by loading on the tensile meridian that are depicted in Fig. 1(a) were also evaluated with the proposed maximum strength criterion, and the corresponding results are plotted in Fig. 23.

It may be observed a good agreement of the peak stresses predicted with the performance dependent criterion, both for NSC and HSC, with available experimental data in almost all the plots in Figs. 17–23.

Nevertheless, the test-data of Ansari and Li (1998) show significant deviations. It is not possible to be conclusive in order to explain the reason of this. On one hand, a cylindrical sample 100 mm/200 mm (diameter/height) was used which is larger than the sample sizes used in most of the other experimental tests being compared. On the other hand, three other differences were noted: (a) cement Type III (ASTM) was used, while cement Type I (ASTM) was used in all the other tests; (b) to limit the effect of the additional confining effect of the rubber membrane on the axial stresses, the obtained concrete strengths were reduced by 7%; and (c) proportional loading was followed.

Example Case 2—The Concrete Mixture Is Unknown and Cannot Be Defined While f_c' Is Known

The Launay and Gachon (1972) triaxial test results are considered in this case. The concrete uniaxial compressive strength is f_c' =36 MPa. However, no information is available regarding the W/B ratio of the concrete mix.

Extreme values of β_P are obtained from Eqs. (5) and (6) for f_c'=36 MPa. They define the following variation range of the performance parameter: $0.063[\beta_P[0.099$. Using the proposed performance dependent maximum strength criterion, the resulting limiting strength curves of the compressive and tensile meridians are depicted in Fig. 24 together with the corresponding experimental results. A very good agreement between experimental and numerical results can be observed in this figure with superior precision in case of the larger β_P. This is probably due to the fact that these tests were performed using a not very effective system to reduce the friction between the sample and the loading platens (aluminum-talc powder sandwich).

Example Case 3—The Concrete Mixture Is Unknown and to Be Defined While f_c' Is Known

Based on the known uniaxial compressive strength f_c', the ANFIS system described in the section called "Evaluation Strategies of the Performance Parameter" is applied. To this end, a concrete mix is proposed and then the uniaxial compressive strength is predicted with the ANFIS system. If the result is acceptable, the mix is selected. If not, another mix proportion is proposed and the process is repeated iteratively. As mentioned in that section, the writers are working on the development of a GAS, based on the ANFIS system, to predict possible concrete mixtures from a given f_c'.

As an example, for f_c'=70 MPa, the mix in Table 1, validated with the ANFIS system is selected:

Then the W/B ratio is calculated, and β_P is determined by means of Eq. (4) leading to β_P=70/0.299/1000=0.234. The plot of the resulting maximum strength curves corresponding to the compressive and tensile meridians for this particular performance parameter and uniaxial compression strength are included in Fig. 25. Observe that if the mixture and the W/B ratio were different, even with the same f_c' different maximum strength curves would be obtained.

In Case 3, corresponding to a concrete to be designed, it is also possible to estimate β_P analogously to case 2, i.e., by means of Eqs. (5) and (6). Nevertheless, the implementation of numerical methods like the ANFIS or the GASs has the advantage to allow a simple and relatively rapid predesign procedure of the concrete mixture right from the beginning of the structural concrete evaluation.

Conclusions

In this paper a performance dependent failure criterion to predict maximum strength of plain concrete is proposed, covering a wide range of concrete qualities, from NSC to HSC. The proposal is based on:

- The so-called "performance parameter" (β_P), that is defined in

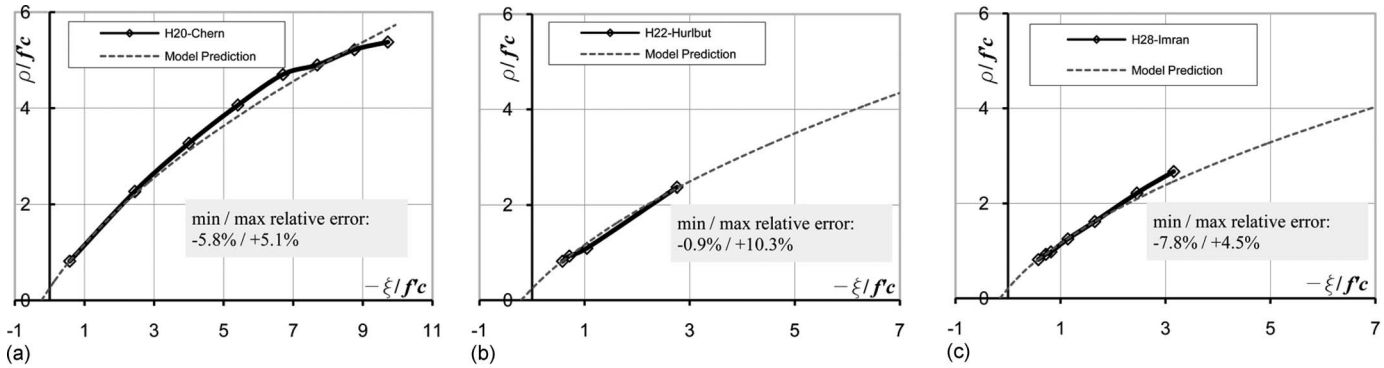

Fig. 17. Numerical prediction of the maximum strength compressive meridian for: (a) $f'_c=20$ MPa; (b) $f'_c=22$ MPa; and (c) $f'_c=28$ MPa

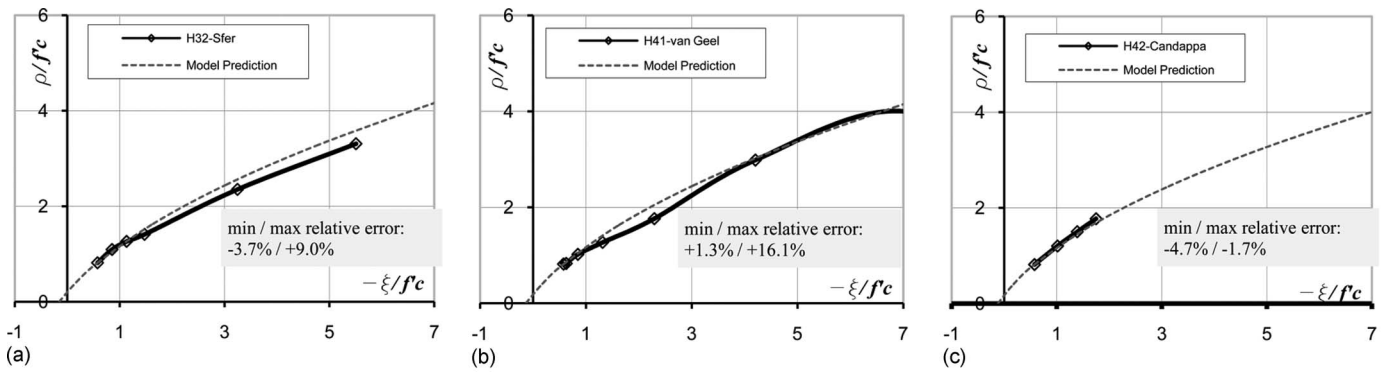

Fig. 18. Numerical prediction of the maximum strength compressive meridian for: (a) $f'_c=32$ MPa; (b) $f'_c=41$ MPa; and (c) $f'_c=42$ MPa

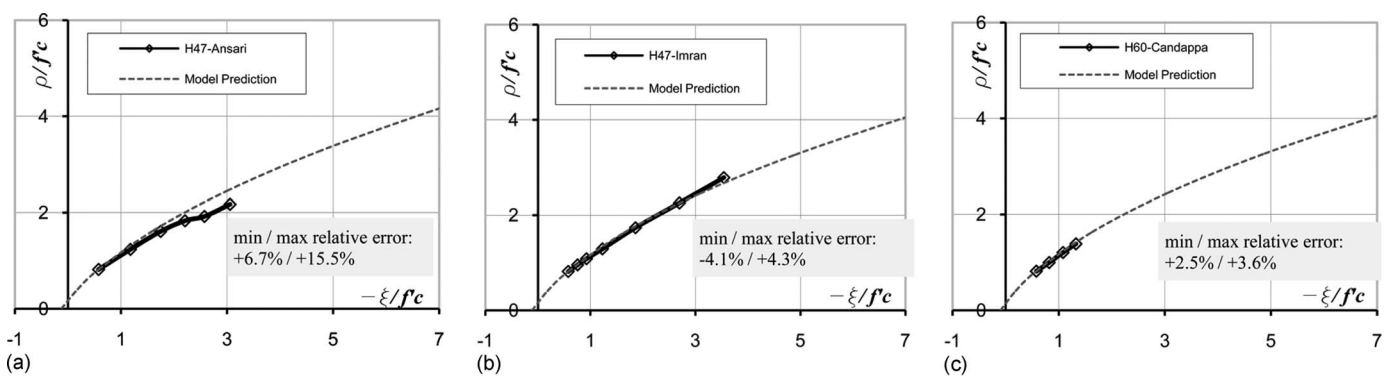

Fig. 19. Numerical prediction of the maximum strength compressive meridian for: (a) $f'_c=47$ MPa; (b) $f'_c=47$ MPa; and (c) $f'_c=60$ MPa

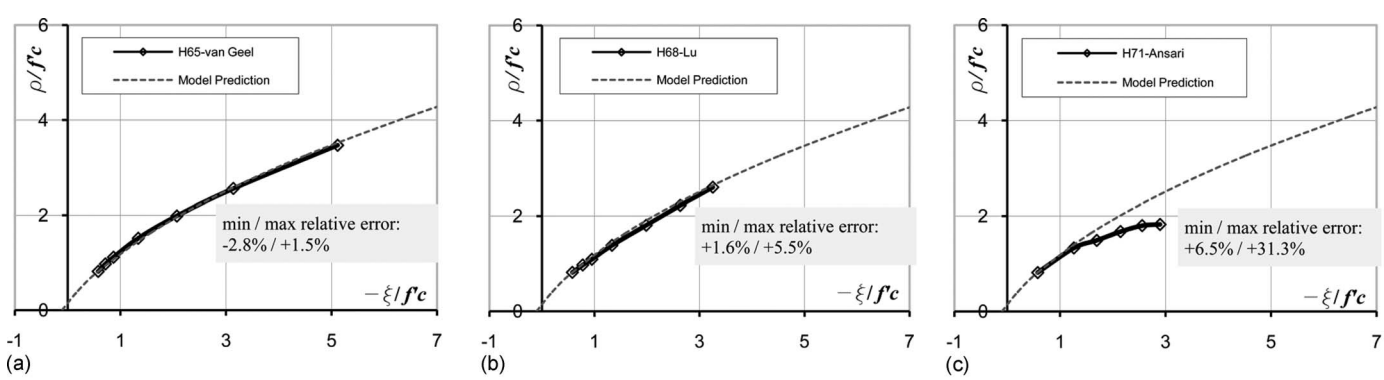

Fig. 20. Numerical prediction of the maximum strength compressive meridian for: (a) $f'_c=65$ MPa; (b) $f'_c=68$ MPa; and (c) $f'_c=71$ MPa

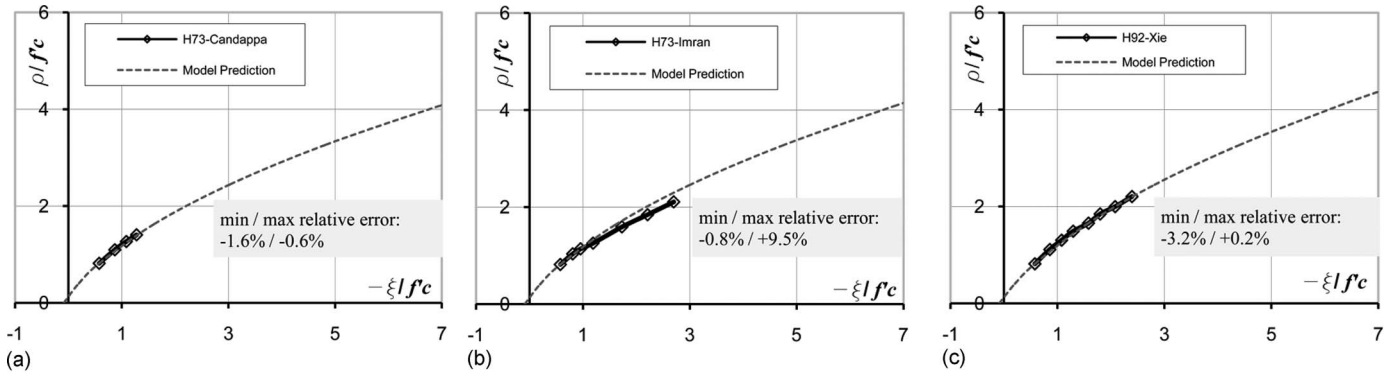

Fig. 21. Numerical prediction of the maximum strength compressive meridian for: (a) $f'_c = 73$ MPa; (b) $f'_c = 73$ MPa; and (c) $f'_c = 96$ MPa

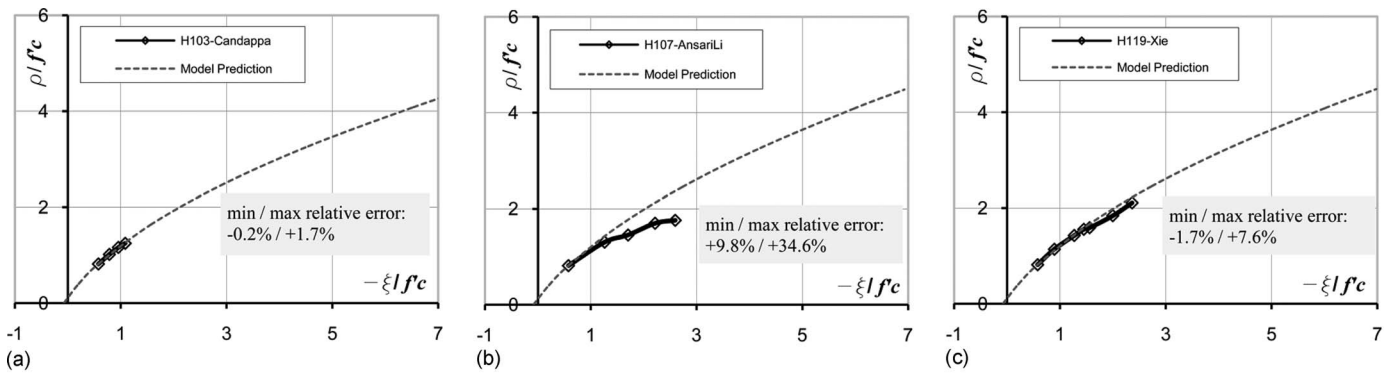

Fig. 22. Numerical prediction of the maximum strength compressive meridian for: (a) $f'_c = 103$ MPa; (b) $f'_c = 107$ MPa; and (c) $f'_c = 114$ MPa

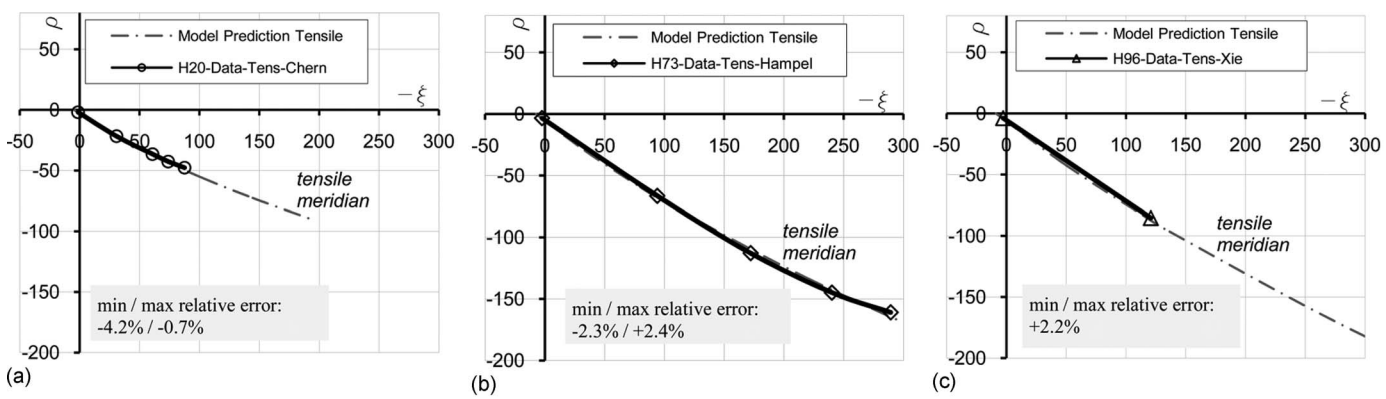

Fig. 23. Numerical prediction of the maximum strength tensile meridian for: (a) $f'_c = 20$ MPa; (b) $f'_c = 73$ MPa; and (c) $f'_c = 96$ MPa

this paper as a depending function of the uniaxial compressive strength f'_c and of the W/B ratio.

- The elliptic interpolation in the deviatoric plane between the compressive and tensile strengths by Willam and Warnke (1974).

The proposed failure criterion for concrete of arbitrary quality reduces to one equation in terms of the three stress invariants, of f'_c and of three material features: the tangent to the compressive meridian at the stress coordinates corresponding to the peak of the uniaxial compressive test, the uniaxial tensile strength ratio and the biaxial compressive strength ratio. These material features are defined as depending functions of the performance parameter and the related functions are also formulated in this proposal. Thus, the failure criterion for concrete of arbitrary quality finally depends on only two controlling material parameters: β_P and f'_c.

The numerical validation analyses in this paper demonstrate good agreement of the peak stresses predicted with the performance dependent criterion, both for NSC and HSC, with available experimental data corresponding to uniaxial, biaxial and triaxial compression tests.

Finally, and in order to assure the feasibility of the solution procedure for any possible set of known data, different numerical methods are presented in this work to evaluate the performance parameter without the need to know the W/B ratio, that is not always available and/or easy to evaluate. For the case of existing concretes, approximation functions are proposed. For the case of concretes to be designed, a method based on an ANFIS system developed previously by the writers is exposed. The ANFIS network details have been published in reference Folino et al. (2007).

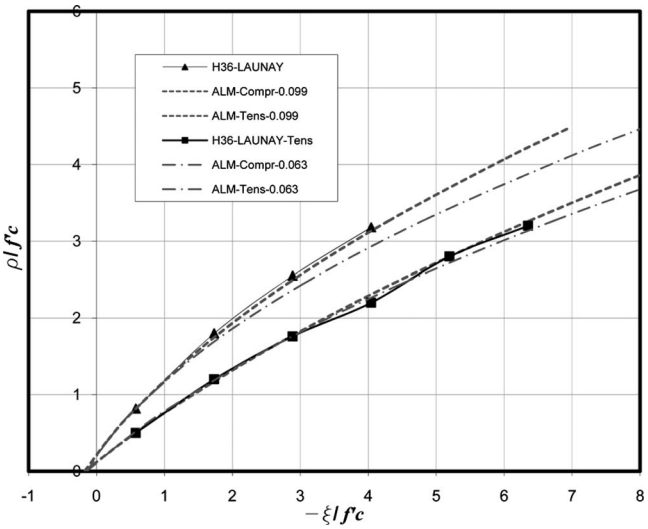

Fig. 24. Maximum strength meridian predictions for the Launay and Gachon (1972) experimental data

Table 1. Selected Concrete Mix Validated with the ANFIS System

Concrete mix constituent	Units	Content
Cement	(kg/m^3)	469
Silica fume	(kg/m^3)	62
Fly ash	(kg/m^3)	0
Water	(kg/m^3)	159
Super plasticizer	(kg/m^3)	7.9
Coarse aggregate	(kg/m^3)	1,100
Fine aggregate	(kg/m^3)	622
Maximum aggregate size	(mm)	12
Coarse aggregate type	—	2
f'_c	(MPa)	70.0

Moreover, the ANFIS network developed in the frame of this work constitutes an interesting tool to be used for the determination of concrete mixtures in the field of concrete technology, regarding the lack of other methods. This network also conduced to the development of a GAS to solve the inverse problem: to obtain different concrete mixes that correspond to a given or desired concrete strength. The details of this GAS are to be published by the writers.

In the future, further research should be perform to extend the presented criterion to take into account other relevant mechanical effects such as time and rate dependence as well as temperature dependence. In this sense, it is convenient to include also chemical effects such as corrosion and alkalis aggregate reactions.

Acknowledgments

The writers gratefully acknowledge the partial financial support of this work by the "Universidad de Buenos Aires," Argentina (UBACYT 2006–2009 Project I813).

Appendix. Determination of the Criterion Coefficients

As detailed in the previous section, to determine the unknown coefficients A, B_c, B_t, and C of the quadratic expressions with common vertex of the compressive and tensile meridians in Eqs. (12) and (13), two constrain conditions are considered to each one of these curves (beside the common vertex). These constrain conditions result from the experimental tests indicated in Fig. 26. As a consequence, the quadratic formulation of the compressive meridian is defined by the common vertex, the stress point corresponding to the peak of the uniaxial compression test, and the inclination of the curve in this stress point. Similarly, the tensile meridian is defined by the common vertex and the stress points

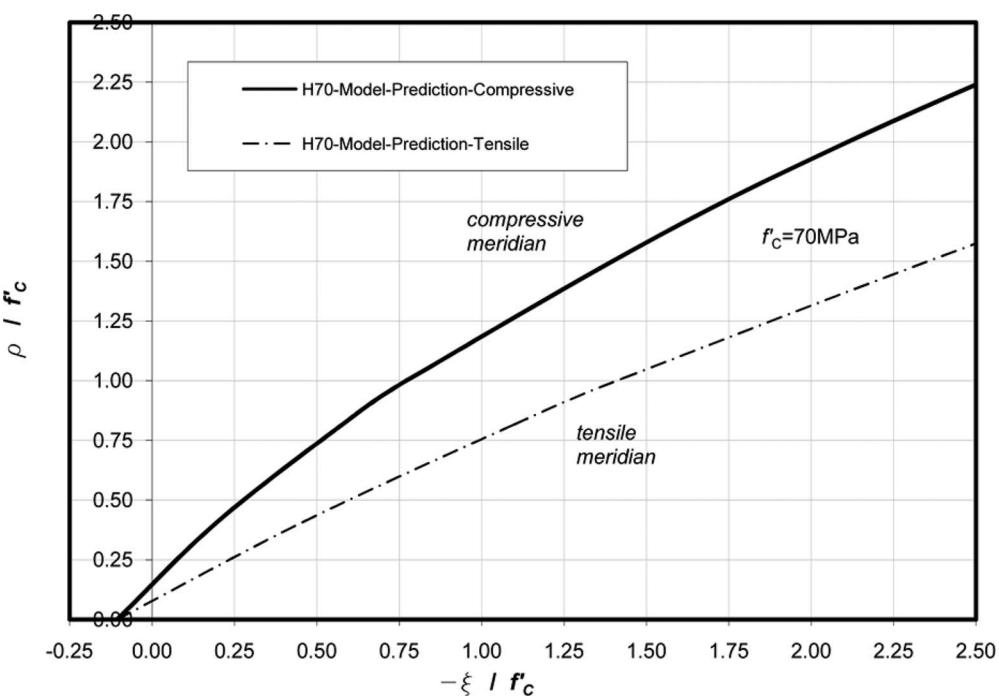

Fig. 25. Predictions of maximum strength meridians for the selected concrete mix

corresponding to the peaks of the uniaxial tensile test and of the CTET with zero axial stress.

Evaluating the imposed conditions to the compressive meridian, result:

Peak of the uniaxial compression test

$$[\underline{\underline{\sigma}}] = \begin{pmatrix} 0 & 0 & 0 \\ 0 & 0 & 0 \\ 0 & 0 & -|f'_c| \end{pmatrix}$$

$$[\underline{\underline{s}}] = \begin{pmatrix} |f'_c|/3 & 0 & 0 \\ 0 & |f'_c|/3 & 0 \\ 0 & 0 & -2|f'_c|/3 \end{pmatrix}$$

$$J_2 = \frac{f'^2_c}{3} \Rightarrow \bar{\rho}_c = \frac{\sqrt{2J_2}}{f'_c} = \sqrt{\frac{2}{3}}$$

$$I_1 = -|f'_c| \Rightarrow \bar{\xi} = \frac{I_1}{\sqrt{3} \cdot f'_c} = -\frac{\sqrt{3}}{3}; \text{ and } \theta = 60°$$

Replacing in Eq. (12)

$$\Rightarrow \frac{2}{3}A + \sqrt{\frac{2}{3}}B_c - \frac{1}{\sqrt{3}}C = 1 \tag{35}$$

Tangent at the peak of the uniaxial compression test

$$\bar{\xi} = \frac{1}{C} \cdot (1 - A \cdot \bar{\rho}_c^2 - B_c \cdot \bar{\rho}_c) \Rightarrow \frac{\partial \bar{\xi}}{\partial \bar{\rho}} = \frac{-2 \cdot A \cdot \bar{\rho}_c - B_c}{C} = -\frac{1}{m}$$

$$\Rightarrow 2 \cdot A \cdot \bar{\rho}_c + B_c - \frac{C}{m} = 0 \Rightarrow 2\sqrt{\frac{2}{3}}A + B_c - \frac{C}{m} = 0 \tag{36}$$

Evaluating the three conditions imposed to the tensile meridian, result:

Peak of the uniaxial tensile test

$$[\underline{\underline{\sigma}}] = \begin{pmatrix} f'_t & 0 & 0 \\ 0 & 0 & 0 \\ 0 & 0 & 0 \end{pmatrix}$$

$$[\underline{\underline{s}}] = \begin{pmatrix} 2f^*_t/3 & 0 & 0 \\ 0 & -f^*_t/3 & 0 \\ 0 & 0 & -f^*_t/3 \end{pmatrix}$$

$$J_2 = \frac{f^{*2}_t}{3} \Rightarrow \bar{\rho}_t = \frac{\sqrt{2 \cdot J_2}}{f'_c} = \sqrt{\frac{2}{3}} \cdot \alpha_t$$

$$I_1 = f^*_t \Rightarrow \bar{\xi} = \frac{I}{\sqrt{3} \cdot f'_c} = \frac{\sqrt{3}}{3}\alpha_t; \text{ and } \theta = 0°$$

Replacing in Eq. (13)

$$\Rightarrow \frac{2}{3} \cdot \alpha_t^2 \cdot A + \sqrt{\frac{2}{3}} \cdot \alpha_t \cdot B_t + \frac{1}{\sqrt{3}} \cdot \alpha_t \cdot C = 1 \tag{37}$$

Peak of the CTET with zero axial stress

$$[\underline{\underline{\sigma}}] = \begin{pmatrix} 0 & 0 & 0 \\ 0 & -|f'_b| & 0 \\ 0 & 0 & -|f'_b| \end{pmatrix}$$

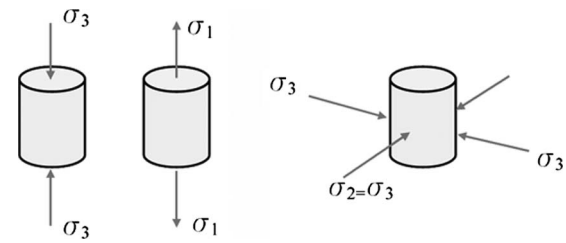

Fig. 26. Uniaxial compression test, uniaxial tensile test, and CTET with zero axial stress

$$[\underline{\underline{s}}] = \begin{pmatrix} \frac{2|f'_b|}{3} & 0 & 0 \\ 0 & -\frac{|f'_b|}{3} & 0 \\ 0 & 0 & -\frac{|f'_b|}{3} \end{pmatrix}$$

$$J_2 = \frac{f'^2_b}{3} \Rightarrow \bar{\rho}_t = \frac{\sqrt{2 \cdot J_2}}{f'_c} = \sqrt{\frac{2}{3}}\alpha_b;$$

$$I_1 = -2|f'_b| \Rightarrow \frac{\xi}{f'_c} = \frac{I_1}{\sqrt{3} \cdot f'_c} = -\frac{2}{\sqrt{3}}\alpha_b; \text{ and } \theta = 90°$$

Replacing in Eq. (13)

$$\Rightarrow \frac{2}{3} \cdot \alpha_b^2 \cdot A + \sqrt{\frac{2}{3}} \cdot \alpha_b \cdot B_t - \frac{2}{\sqrt{3}} \cdot \alpha_b \cdot C = 1 \tag{38}$$

Eqs. (35)–(38) constitute a system of four linear equations with four unknowns. The explicit expressions of the coefficients A, B_c, B_t, and C, given in Eqs. (18)–(21), are obtained from the solution of this system of equations.

The equations defining the proposed performance dependent failure criterion are summarized as follows:

$$\forall \quad 0° \leq \theta \leq 60°$$

$$F_{(\bar{\xi},\bar{\rho},\theta,f'_c,\beta_P)} = A \cdot r^2 \cdot \overline{\rho^{*2}} + B_c \cdot r \cdot \overline{\rho^*} + C \cdot \bar{\xi} - 1 = 0 \tag{39}$$

with

$$r_{(\bar{\xi},\theta,f'_c,\beta_P)} = \frac{4(1-e^2)\cos^2\theta + (2e-1)^2}{2(1-e^2)\cos\theta + (2e-1)\sqrt{4(1-e^2)\cos^2\theta + 5e^2 - 4e}}$$

$$e_{(\bar{\xi},f'_c,\beta_P)} = \frac{-B_t + \sqrt{B_t^2 + 2 \cdot A \cdot \overline{\rho_c} \cdot (2 \cdot A \cdot \overline{\rho_c} + 2 \cdot B_c)}}{2 \cdot A \cdot \overline{\rho_c}} \tag{40}$$

where

$$\overline{\rho_c}_{(\bar{\xi},f'_c,\beta_P)} = \frac{-B_c + \sqrt{B_c^2 + 4 \cdot A \cdot (1 - C \cdot \bar{\xi})}}{2 \cdot A}$$

$$\Rightarrow e_{(\bar{\xi},f'_c,\beta_P)} = \frac{-B_t + \sqrt{B_t^2 + 4 \cdot A \cdot (1 - C \cdot \bar{\xi})}}{-B_c + \sqrt{B_c^2 + 4 \cdot A \cdot (1 - C \cdot \bar{\xi})}} \tag{41}$$

$$A_{(f'_c,\beta_P)} = -\frac{3}{2}\left\{1 + \frac{(m-\sqrt{2})(1-\alpha_b\alpha_t)(\alpha_b-\alpha_t)}{\alpha_b\alpha_t[(m-\sqrt{2})(\alpha_b-\alpha_t)+3m]}\right\} \quad (42)$$

$$B_{c(f'_c,\beta_P)} = -\sqrt{3}\left\{\sqrt{2} + \frac{(\sqrt{2}m-1)(1-\alpha_b\alpha_t)(\alpha_b-\alpha_t)}{\alpha_b\alpha_t[(m-\sqrt{2})(\alpha_b-\alpha_t)+3m]}\right\} \quad (43)$$

$$B_{t(f'_c,\beta_P)} = -\sqrt{\frac{3}{2}}\left\{\frac{1+\alpha_t^2}{\alpha_t} + \frac{[(m-\sqrt{2})\alpha_t - m](1-\alpha_b\alpha_t)(\alpha_b-\alpha_t)}{\alpha_b\alpha_t[(m-\sqrt{2})(\alpha_b-\alpha_t)+3m]}\right\} \quad (44)$$

$$C_{(f'_c,\beta_P)} = -\sqrt{3}m\frac{(1-\alpha_b\alpha_t)(\alpha_b-\alpha_t)}{\alpha_b\alpha_t[(m-\sqrt{2})(\alpha_b-\alpha_t)+3m]} \quad (45)$$

Finally, three predictions of the compressive meridian of the failure surface obtained with the proposed maximum strength criterion, and for concretes of three different qualities are presented. In all the three cases, the performance parameter β_P considered was the mean value between the upper and lower limits evaluated by Eqs. (5) and (6)

$$(1)\ f'_c = 20\ \text{MPa};\ \beta_P = 0.031$$

$$-\bar{\xi} = 0.173\cdot\bar{\rho}^2 + 0.851\cdot\bar{\rho} - 0.232$$

$$(2)\ f'_c = 60\ \text{MPa};\ \beta_P = 0.179$$

$$-\bar{\xi} = 0.232\cdot\bar{\rho}^2 + 0.659\cdot\bar{\rho} - 0.115$$

$$(3)\ f'_c = 120\ \text{MPa};\ \beta_P = 0.803$$

$$-\bar{\xi} = 0.182\cdot\bar{\rho}^2 + 0.665\cdot\bar{\rho} - 0.087$$

Notation

The following symbols are used in this paper:

$A;B_c;B_t;C$ = coefficients in the performance dependent failure criterion equation;
e = eccentricity$=\rho_t/\rho_c$;
f'_b = peak lateral confining pressure of the CTET under zero axial stress or biaxial compressive strength (MPa);
f^*_b = proposed peak lateral confining pressure of the CTET under zero axial stress or biaxial compressive strength calibrated in terms of β_P (MPa);
f'_c = uniaxial compressive strength (MPa);
f'_t = uniaxial tensile strength (MPa);
f^*_t = proposed uniaxial tensile strength calibrated in terms of β_P (MPa);
I_1 = first invariant of the stress tensor (MPa);
J_2 = second invariant of the deviatoric stress tensor (MPa^2);
J_3 = third invariant of the deviatoric stress tensor (MPa^3);
m = material parameter representing the friction property empirically calibrated in terms of β_P;
$\underline{\underline{s}}$ = deviatoric stress tensor (components s_{ij}) (MPa);
W/B = water/binder ratio [W=water content(kg/m^3)], B=(cement +mineral admixtures) contents (kg/m^3);
α_b = compressive strength ratio f^*_b/f'_c;
α_t = tensile strength ratio f^*_t/f'_c;
β_P = performance parameter;
δ_{ij} = Kronecker delta ($\delta_{ij}=1$ if $i=j$; $\delta_{ij}=0$ if $i\gamma j$);
$\xi;\rho;\theta$ = Haigh Westergaard coordinates in the principal stress space (MPa);
$\bar{\rho};\bar{\xi}$ = normalized first and second Haigh Westergaard coordinates in the principal stress space;
ρ^* = shear strength (Haigh Westergaard second coordinate) (MPa);
ρ_c = Haigh Westergaard second coordinate for $\theta=\pi/3$ (compressive meridian) (MPa);
ρ_t = Haigh Westergaard second coordinndate for $\theta=0$ (tensile meridian) (MPa);
$\underline{\underline{\sigma}}$ = Cauchy stress tensor (components σ_{ij}) (MPa); and
$\Phi_{\max}$ = maximum coarse aggregate (mm).

References

Ansari, Q. and Li, Q. (1998). "High-strength concrete subjected to triaxial compression." *ACI Mater. J.*, 95(6), 747–755.

Candappa, D. C., Sanjayan, J. G., and Setunge, S. (2001). "Complete triaxial stress-strain curves of high-strength concrete." *J. Mater. Civ. Eng.*, 13(3), 209–215.

Chern, J., Yang, H., and Chen, H. (1992). "Behavior of steel fiber reinforced concrete in multiaxial loading." *ACI Mater. J.*, 89(1), 32–40.

Drucker, D. C., and Prager, W. (1952). "Soil mechanics and plastic analysis of limit design." *Brown University, Quarterly of Applied Mathematics*, 10, 157–165.

Etse, G. (1992). "Theoretische und numerische untersuchung zum diffusen und lokalisierten Versagen in Beton." Ph.D. thesis, Univ. of Karlsruhe, Karlsruhe, Germany.

Etse, G. and Willam, K. (1994). "Fracture energy formulation for inelastic behavior of plain concrete." *J. Eng. Mech.*, 120(9), 1983–2011.

Folino, P., Will, A., Flores, F., Diaz, W., and Etse, G. (2007). "Uso de redes neuronales y ANFIS para predecir la resistencia uniaxial a compresión de hormigones de alta resistencia." *Proc. ENIEF 2007, Mecánica Computacional*, Vol. XXVI, AMCA, Argentina, 1413–1426.

Hampel, T. and Curbach, M. (2000). "Behavior of high performance concrete under biaxial and triaxial compression." *Proc., 3rd Int. Ph.D.—Symp. in Civil Engineering*, FIB.

Hoek, E., and Brown, E. T. (1980). "Empirical strength criterion for rock masses." *J. Geotech. Engrg. Div.*, 106(9), 1013–1035.

Hurlbut, B. J. (1985). "Experimental and computational investigation of strain-softening in concrete." MS thesis, University of Colorado, Boulder.

Hussein, A. and Marzouk, H. (2000). "Behavior of high-strength concrete under biaxial stresses." *ACI Mater. J.*, 97(1), 27–36.

Imran, I. and Pantazopoulou, S. J. (1996). "Experimental study of plain concrete under triaxial stress." *ACI Mater. J.*, 93(6), 589–601.

Launay, P. and Gachon, H. (1972). "Strain and ultimate strength of concrete under triaxial stress." *ACI Special Publication, SP 34, Paper 13*, 269–283.

Leon, A. (1935), "Über die Scherfestigkeit des Betons (Over the shearing strength of concrete)." *Beton und Eisen*, Vol. 34-8, Berlin.

Lu, X. (2005). "Uniaxial and triaxial behavior of high strength concrete

with and without steel fibers." Ph.D. thesis, New Jersey Institute of Technology.

Mohr, O. (1900). "Welche Umstande bedingen die Elastizitatsgrenze und den Bruch eines Materials." *Zeitschrift des Vereins Deutscher Ingenieure Band*, 44, 1524–1530.

Ottosen, N. S. (1977). "A failure criterion for concrete." *J. Eng. Mech. Div.*, 103(EM4), 527–535.

Rankine, W. J. M. (1876). "A manual of applied mechanics." *C. Griffin and Co. (London)*.

Schleicher, F. (1926). "Der Spannungszustand an der Fliessgrenze (Plastizitätsbedingung)." *Z. Angew. Math. Mech.*, 6, 199–216.

Seow, P. and Swaddiwudhipong, S. (2005). "Failure surface for concrete under multiaxial load—A unified approach." *J. Mater. Civ. Eng.*, 17(2), 219–228.

Sfer, D., Carol, I., Gettu, R., and Etse, G. (2002). "Experimental study of the triaxial behavior of concrete." *J. Eng. Mech.*, 128(2), 156–163.

van Geel, E. (1998). "Concrete behavior in multiaxial compression." Doctoral thesis, Technische Universiteit Eindhoven.

von Mises, R. (1926). "Fluglehre. Vortrage über Theorie und Berechnung der Flugzeuge in elementarer Darstellung." *3te, stark erweiterte Auflage*, Springer, Berlin, 6–321.

Willam, K. J., and Warnke, E. P. (1974). "Constitutive model for the triaxial behavior of concrete." *Proc., Int. Association of Bridge and Structural Engineering, Rep. 19, Section III*, IABSE, Zurich, Switzerland, 1–30.

Xie, J., Elwi, A., and Mac Gregor, J. (1995). "Mechanical properties of three high-strength concretes containing slica fume." *ACI Mater. J.*, 92(2), 135–145.